Journal of The Electrochemical Society, **150** (3) C115-C124 (2003)
0013-4651/2003/150(3)/C115/10/$7.00 © The Electrochemical Society, Inc.

Correlation of Film Structure with Film Formation in Cationic Electropaint Systems

An Ionically Conductive Model

Yo-ichiro Suzuki,[a,b,*,z] Hirokazu Fukui,[a] Kazuyo Tsuchiya,[a] Satoru Arita,[a] and Yukio H. Ogata[b,*]

[a]*C. Uyemura & Co., Ltd., Central R & D Lab, Hirakata, Osaka 573-0065, Japan*
[b]*Institute of Advanced Energy, Kyoto University, Uji, Kyoto 611-0011, Japan*

Using two cationic electropaint resins, the deposition mechanism including the film structure was studied. The resins introduced methyl methacrylate (MMA system) or methyl acrylate (MA system) into a backbone component, and these systems showed different values of the glass transition temperature (T_g). The MMA resin had a T_g of 70°C, and the MA resin 5°C. A film was deposited under conditions of both constant voltage and constant current, and the film resistivity was estimated. The surface of the deposited film was also observed by scanning electron microscopy (SEM). For the MMA, the film resistivity was on the order of 10^8 Ω cm. The MMA formed a dense film as the first layer at the start of deposition, and the electrochemical behavior of the film depended on the electrolysis conditions: constant voltage or constant current deposition. The voltage-current curves for the MMA film exhibited a nonohmic behavior. SEM images of the MMA film thinner than 30 μm revealed that pores up to 0.5 μm diam were scattered in the film. Moreover, by increasing the thickness, the film morphology was transformed into a spongy layer with holes up to several mm diam. However, the resistivity of the MA film was almost constant during deposition, and it was on the order of 10^7 Ω cm or less. The voltage-current curves for the MA showed an ohmic behavior. The MA film was nonporous, and such a structure was maintained up to 25 μm thick. As the thickness increased, the deposition morphology was also transformed into a spongy layer from a nonporous layer. The resistivity of both films depended on the concentration of lactic acid in the film and on the morphology of the deposits. We clarified that the film formation mechanism of both systems was similar. A new model proposed as the mechanism is that of ion-permeable film formation.
 [DOI: 10.1149/1.1541674]

Manuscript submitted February 14, 2002; revised manuscript received August 26, 2002. Available electronically January 28, 2003.

A deposited film in an electropaint system has high electric resistance. The film characteristics enable a complicated-shaped surface to be covered with a film having a high throwing power. The throwing power plays an important role in improving the corrosion resistance of metals. A tube test is one evaluation technique for the throwing power. Furuno *et al.* used the tube test to analyze an electropaint system, and they reported that high film resistance, as well as high conductivity of a resin solution, produces a high throwing power.[1,2] It is easy to raise the solution conductivity by adding a neutralizer. High neutralization promotes hydrolysis of the resin solution and/or causes film defects by electrolytic gases, leading to pinhole problems and film ruptures. Therefore, controlling the film resistance during deposition is a better option for improving the throwing power. In addition, understanding what governs the film resistance gives important information in regard to improving the throwing power.

We have reported the influence of the glass transition temperature (T_g) of resins on deposition behavior, using two cationic resins with different T_g values as model resins.[3] We found that the film resistivity depended on the T_g and that there were two types of film formation. A resin with high T_g shows high resistance film formation (HRFF) behavior, while a resin with low T_g follows the ion-permeable film formation (IPFF) mechanism. The former produces a high resistance film, and the latter behaves as a conductive film. Observations with an atomic force microscope (AFM) show that the HRFF produces a layer on which resin particles are piled, and that the IPFF creates a layer having a flat surface without any particles.[3,4] The T_g changes the film morphology.

In general, many works have supported the porous film (PF) model:[5,6] in this model, mass transport and current flow take place through the pores formed in the film during deposition. We made it clear that the film growth progresses at the film/solution interface.[3,4] However, this PF model cannot perfectly account for some experimental results. Therefore, we must reconsider the correlation of the formation mechanism with the film structure.

The purpose here is to investigate this correlation to understand the change in the film resistivity during deposition. Although there are two types of film formation, HRFF and IPFF, both formations turned out to be practically the same. A new model is proposed to explain the film formation mechanism. Moreover, it is revealed that not only the concentration of lactic acid in the film but also the film structure affect the film resistivity during deposition.

Experimental

A cationic acrylic resin was synthesized by radical polymerization. Lactic acid and deionized water were mixed in the resin to prepare a resin solution of 10% in solid concentration. Preparation of the resin and its solution has been reported in our previous paper.[3,4] The resins used in these experiments were of two types, introducing methyl methacrylate (MMA) or methyl acrylate (MA) as a backbone component. The resin system that introduced MMA has a T_g of 70°C (MMA system), and the resin system introducing MA has a T_g of 5°C (MA system). The two systems are hereafter denoted by MMA and MA, respectively. The solid concentration, conductivity, and milliequivalents of the resin solution were determined.[4] A Cu-Zn alloy plate (65% Cu-35% Zn) was used as a cathode (210 cm^2 surface area). The counter electrode was a 304 stainless steel plate of 105 cm^2 and was separated 60 mm from the cathode. Electrodeposition was performed under constant voltage or current conditions. After being rinsed with water, the deposited film was dried for weighing with an electric balance. Conditions for deposition were as follows: the bath temperature was 25°C, the applied voltage was varied from 2 to 150 V, the current density was 0.2-1.0 mA/cm^2, and the deposition time was 10-2000 s. A model IPS-0120-3 (120 V, 3 A; Takasago Power Supply) power source was mainly used, and a combination of AP-EC01 and GP-0650 (650 V, 5 A; Takasago Power Supply) was also used. For the potentiodynamic experiments, a high potential-type potentiostat (350 V, 5 A; Hokuto

* Electrochemical Society Active Member.
z E-mail: yoichiro-suzuki@uyemura.co.jp

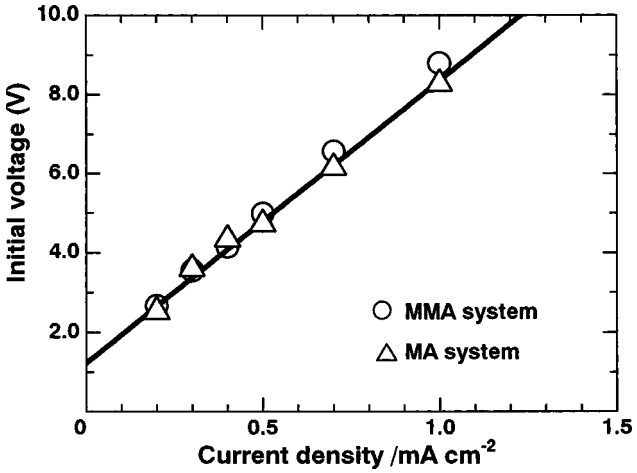

Figure 1. Relationship between current density and initial voltage. The data were obtained from the MMA and the MA solutions under constant current deposition. The conductivity was 659 μS/cm for the MMA and 727 μS/cm for the MA at 25°C.

Denko) was used. Surface observation of deposited films was performed using scanning electron microscopy (SEM, JEOL model JSM-5600).

The conductivity of the resin solution used in these experiments was 659 μS/cm for the MMA and 727 μS/cm for the MA. Both solutions had similar conductivities. Because of the low conductivity, the ohmic drops of a solution and a deposited film govern the voltage balance during electrodeposition. According to Ohm's law, under constant voltage deposition, the resistivity of a film, ρ_F, is given by

$$\rho_F = \frac{1}{L_F}\left(\frac{E}{i} - \rho_S L_S\right) = \frac{E}{L_F}\left(\frac{1}{i} - \frac{1}{i_0}\right) \quad [1]$$

where E is the voltage (V), i the current density (mA/cm^2), ρ the resistivity (Ω cm), L_F the film thickness (cm), and L_S the electrode separation (cm). The subscript F denotes the film, and the subscript 0 at time = 0. Under constant current conditions, Eq. 2 is obtained

$$\rho_F = \frac{1}{L_F}\left(\frac{E}{i} - \rho_S L_S\right) = \frac{1}{iL_F}(E - E_0) \quad [2]$$

The film resistivity was calculated by using Eq. 1 and 2 from the experimental data. We presuppose that these equations are applied to a film thicker than 0.5 μm.

Results

Resistivity of resin solution.—Solution resistivity was evaluated by measuring the response immediately after voltage or current was applied to the systems. Under constant voltage deposition, the initial current was proportional to the applied voltage, and Ohm's law was satisfied. The ohmic relationship was also satisfied under constant current deposition (Fig. 1). The solution resistivity for both systems was estimated to be about 1.2×10^3 Ω cm.

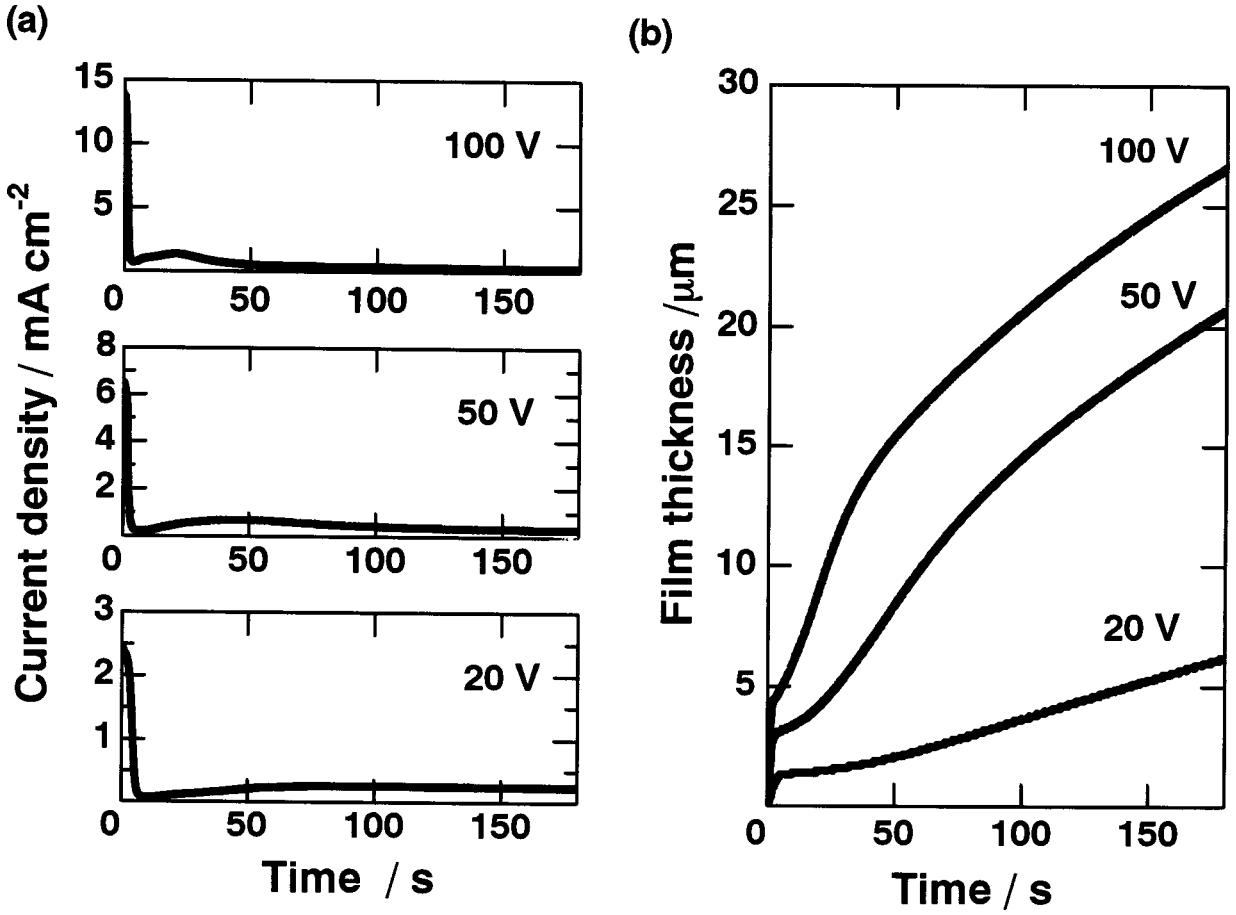

Figure 2. (a) Current-time curves the MMA film was deposited at various voltages for 180 s. (b) Time dependence of the film thickness obtained from the current-time curves.

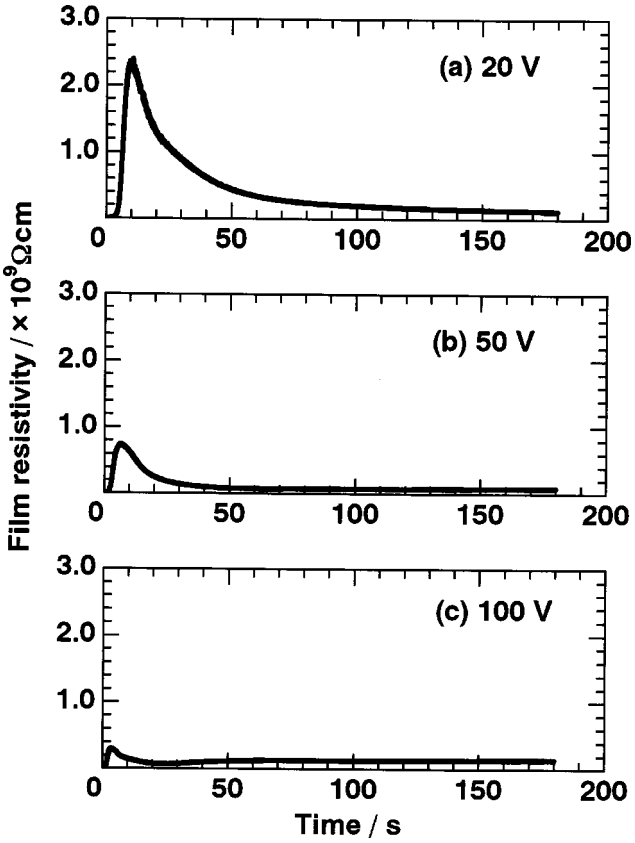

Figure 3. Change in film resistivity of the MMA deposited at various voltages as a function of deposition time. Resistivity was calculated using Eq. 1.

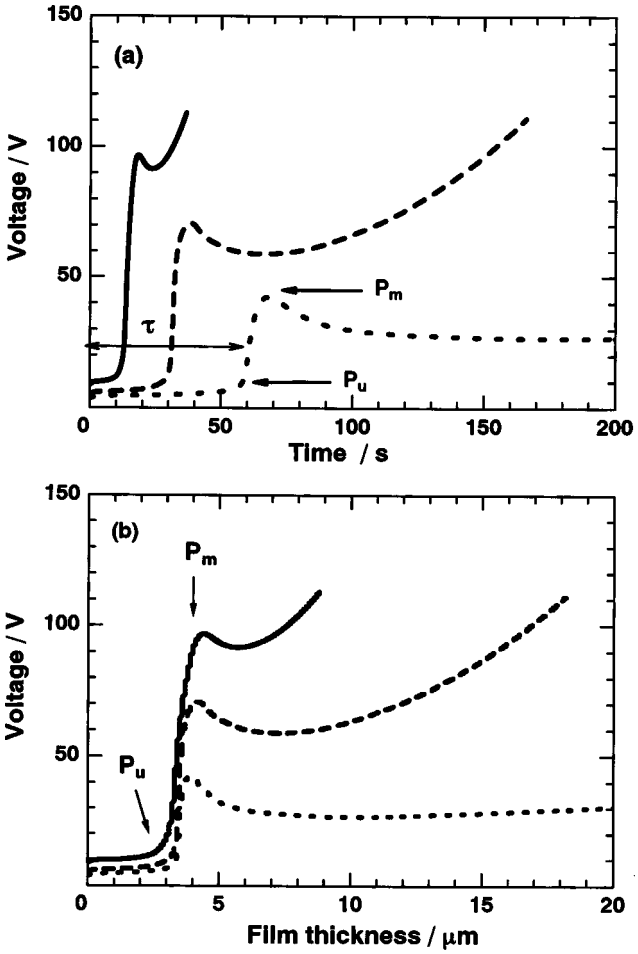

Figure 4. (a) Voltage-time curves the MMA film was deposited at various current densities. (b) Correlation of voltage with film thickness obtained from the voltage-time curves. Dotted line shows 0.3 mA/cm^2; dashed line, 0.5 mA/cm^2; and solid line, 1.0 mA/cm^2. τ is the induction period.

Film deposition from the MMA system.—Deposition behavior at constant voltage.—Figure 2a gives the current-time curves when the MMA film was deposited at constant voltage. An abrupt decrease in current indicates the HRFF. Applying a voltage higher than 20 V for 180 s could deposit a dense film of 10-20 μm, a thickness that satisfies the practical requirements. The initial current density changed from 2.5 to 14 mA/cm^2, depending upon the voltage. Further electrolysis (180 s or more) did not give a film thicker than 30 μm, even for an applied voltage of 150 V. No film rupture was observed during electrodeposition. The deposit weight of a film is proportional to the number of coulombs passed during electrolysis. Thus, the deposit weight can be estimated from the current-time curve and gives good agreement with the measured data.[3] Figure 2b shows the time dependence of the film thickness, where a density of 1 g/cm^3 was used for the MMA film to convert deposit weight into thickness. The thickness increased most abruptly at the early stage, and then increased moderately with time. When electrolysis of water occurs at high current density in the period from the start of deposition to the end of the abrupt fall in current, a film thickness of only 15-20% of the total is deposited. The film essentially grows at a low current density after the current decreases abruptly in the current-time curve.

The film resistivity of the MMA was calculated using Eq. 1. The time dependence is shown in Fig. 3. The resistivity increased abruptly and formed a peak (a maximum). After that, the film resistivity decreased gradually. The resistivity at the peak was 10^8-10^9 Ω cm. The influence of thickness on the film resistivity was checked. At 20 V, the resistivity increased suddenly at 1.0 μm thick, and then the peak appeared at 1.5 μm. As the applied voltage was increased, the thickness giving the peak increased: 3.3 μm at 50 V and 4.5 μm at 100 V. The resistivity approached the order of 1×10^8 Ω cm when the thickness exceeded 6 μm. At this stage, the resistivity no longer depended on the voltage.

Deposition behavior at constant current.—Electrodeposition of the MMA was performed at constant current (in the maximum range of 120 V), and voltage-time curves were measured (Fig. 4). The voltage increased abruptly after an induction period τ (stagnant period) of several tens of seconds at the point P_u, and then the peak appeared at the point P_m (Fig. 4a). The lower the current density was, the longer the induction period became. The voltage peak became small with decreasing current density. The time reaching 120 V was about 2000 s at 0.2 mA/cm^2 and about 500 s at 0.3 mA/cm^2. In the current density range of 0.5-1.0 mA/cm^2, it took 40-160 s to reach 120 V, as can be seen in Fig. 4a. For the constant current deposition, the forced current flow enables a thickness of 30 μm or more to be deposited. The deposited film was observed with an optical microscope. After exceeding 30 μm in thickness, the film was transformed into a spongy layer. The spongy layer had holes rather than pores, and the size was distributed from 0.1 to 3 mm diam. A film rupture for the MMA took place at 240-280 V, and the voltage was independent of the applied current density. Once the film rupture was initiated, the film was observed with the optical microscope. The film rupture took place within the film. Segments of the film broke down and floated on the solution surface, while the remaining film on the substrate was as dense as the film thinner than 30 μm. After the rupture voltage was reached, the voltage oscillated with repeated destruction and restoration of the deposited film. In addition, the

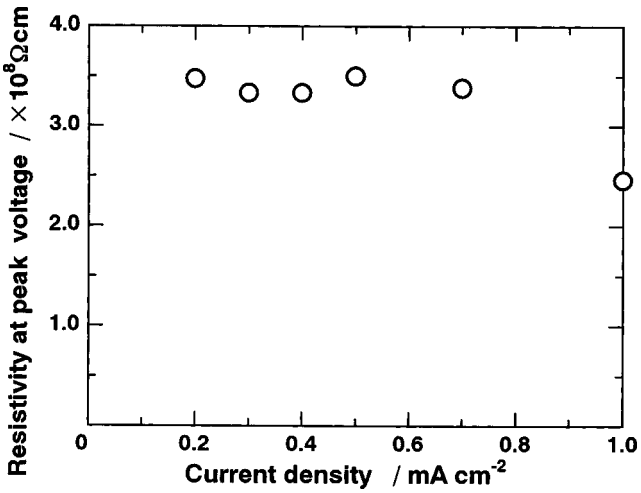

Figure 5. Relationship between current density and resistivity at peak voltage (the point P_m shown in Fig. 4). Data were obtained from the MMA under constant current deposition.

solution temperature rose gradually just before reaching the rupture voltage.

Under constant current deposition, the deposit weight (or the thickness) of the film is also proportional to the number of coulombs passed. A change in voltage as a function of the deposited film thickness is plotted in Fig. 4b. The results show that an abrupt rise in voltage occurred at about a thickness of 3 μm, and a voltage peak appeared at about 4 μm. The resistivity of the MMA film was estimated using Eq. 2. The correlation of thickness with resistivity shows that a peak of the resistivity was also formed at about 4 μm corresponding to the point P_m in Fig. 4b. Figure 5 gives the dependence of current density on the resistivity at each peak. The resistivity at the peak was about 3.5×10^8 Ω cm in the range of 0.2-0.7 mA/cm^2 and 2.5×10^8 Ω cm at 1.0 mA/cm^2. The resistivity is almost independent of current density. A film of cationic electropaint is deposited by electrolysis of water at a cathode. It has been believed that the disperse particles of resin initiate coagulation after hydroxide ions produced at the cathode reach a critical concentration during the induction period.[5-8] However, our AFM observations revealed that the disperse particles can coagulate even during the induction period.[4] Therefore, the induction period should be defined as the time when the film reaches a certain resistivity.

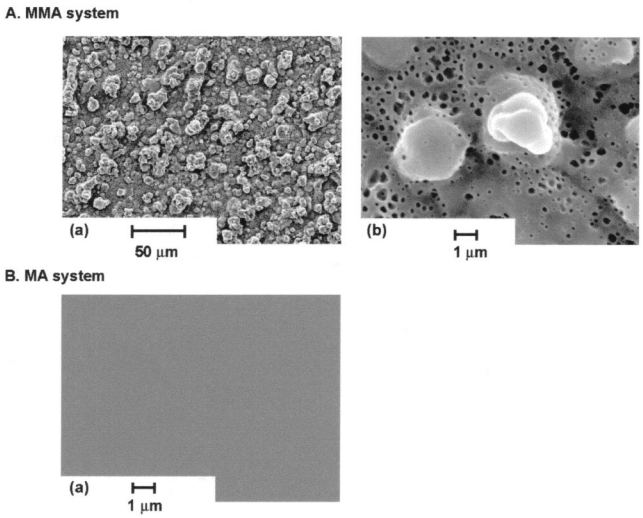

Figure 6. SEM images of (A) the MMA and (B) the MA. The films were deposited at 0.5 mA/cm^2 for 90 s.

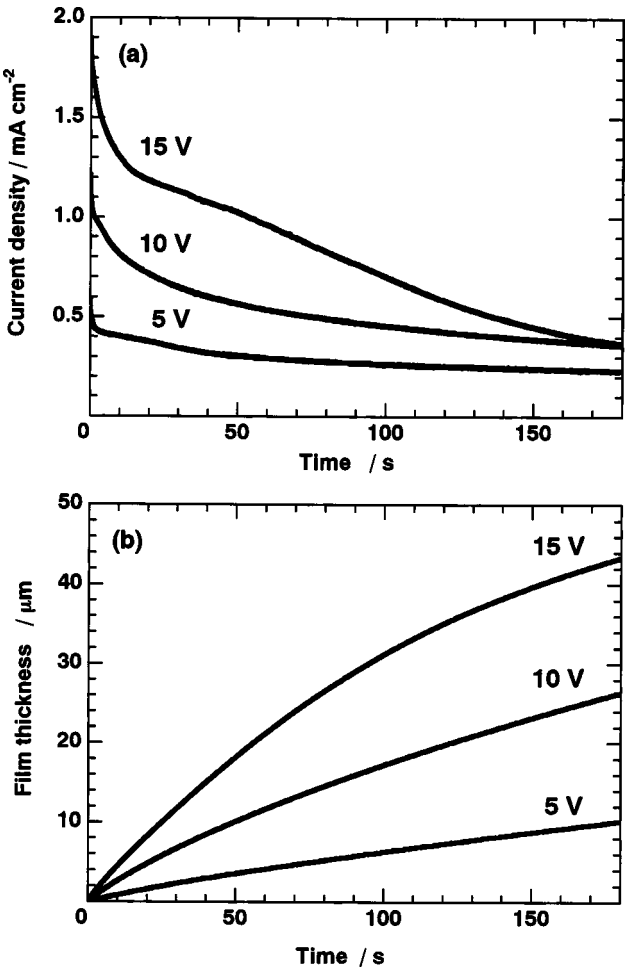

Figure 7. (a) Current density-time curves where the MA film was deposited at various voltages for 180 s. (b) Time dependence of the film thickness obtained from the current-time curves.

Film observation.—The MMA film up to 25 μm was relatively dense under both conditions of constant voltage and current when seen with the naked eye. Such a film was observed using SEM. Similar images were obtained in the film surfaces irrespective of the deposition modes. Figure 6 shows SEM images of the MMA film deposited at 0.5 mA/cm^2 and for 90 s. Aggregates and pores can be observed on the film surface. The aggregates were 10-20 μm in size [Fig. 6A(b)]. As shown in this figure, the pore size was 0.01-0.5 μm diam, and pores could be also seen on the surface of the aggregates. The AFM images for the MMA film showed resin particles constituting the aggregates.[3,4] However, we were unable to observe them by SEM, probably because the film would suffer damages due to the heat of the electron beam and the high vacuum. Although the SEM images may support the PF model, our results cannot be fully explained.

Deposition of the MA film.—When the MA film was electrodeposited in the range of 5-15 V, the current density at the early stage was 0.6-1.8 mA/cm^2. The current decreased monotonously with time from the start of deposition (Fig. 7a). Furthermore, even at such a low voltage, the MA could produce a film as thick as the MMA (Fig. 7b). The thickness increased gradually from the start. The MA film had a low rupture voltage in comparison with the MMA, and the film rupture took place at voltages higher than 50 V.

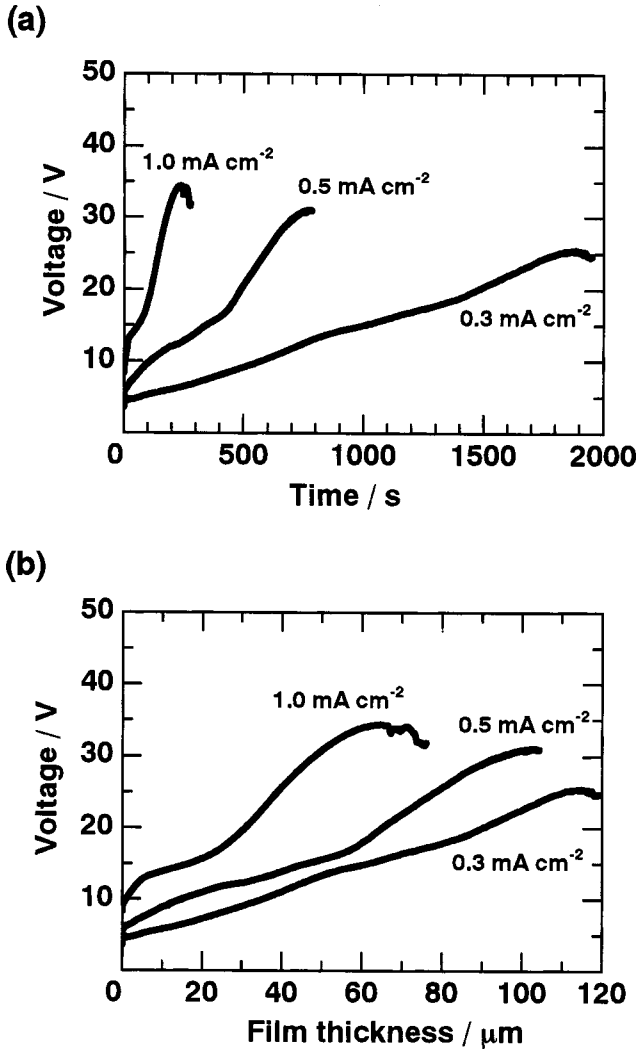

Figure 8. (a) Voltage-time curves where the MA film was deposited at various current densities. (b) Correlations of voltage with film thickness obtained from the voltage-time curves.

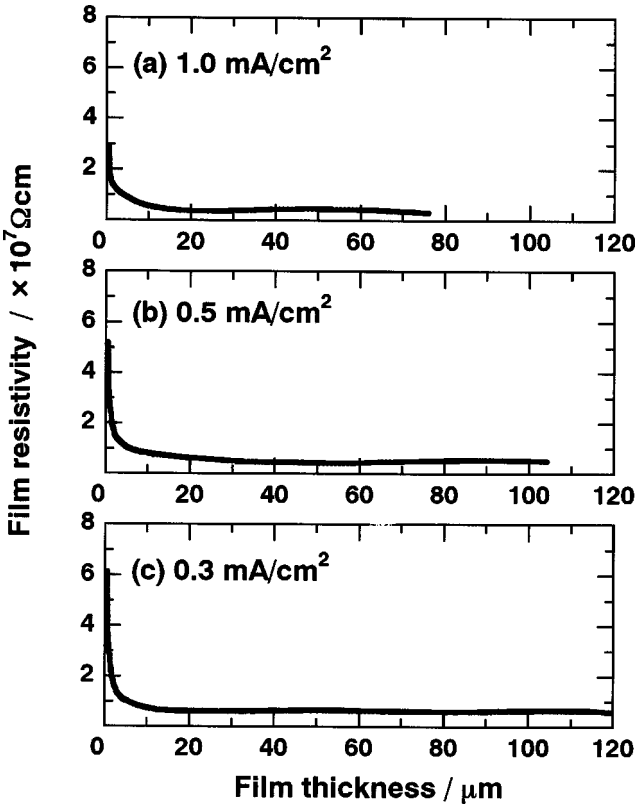

Figure 9. Change in film resistivity of the MA deposited at various current densities as a function of deposition time. The resistivity was calculated using Eq. 2.

Figure 8a shows the voltage-time curves for the MA under constant current deposition. At a current density of 0.3 mA/cm^2 and for a deposition time of 2000 s, the voltage gradually increased from 5 to 25 V. The rate of the rise in voltage was very slow even if the current density increased. Unlike the MMA, an abrupt rise in voltage did not appear. Figure 8b gives the change in voltage as a function of thickness. The increase in voltage was almost proportional to the thickness. Reaching a thickness of 60-120 μm caused a film rupture, and the rupture voltage was in the range of 25-35 V.

The MA films deposited under both deposition conditions were observed using SEM. The images of the film up to 30 μm showed a flat surface without any characteristic surface structures [Fig. 6B(a)]. Such films appeared to be dense by naked eye observation. Observation with an optical microscope showed that the film thicker than 30 μm was transformed into a spongy layer similar to that of the MMA. The film rupture occurred inside the MA film, like the MMA. A part of the spongy layer was peeling off, and the remaining film on the substrate had a denseness similar to that of the MA film of 30 μm or less.

The estimation of resistivity for the MA film revealed similar changes irrespective of the deposition modes. The resistivity was 3-6 $\times$ 10^7 Ω cm at the early stage of deposition and approached a value of 0.2-1.8 $\times$ 10^7 Ω cm during the film growth. Under constant current deposition, Fig. 9 gives the change in resistivity, which was calculated according to Ohm's law, as a function of the film thickness. The rapid falls in film resistivity ranged up to 5 μm thick, and then the resistivity gradually decreased and remained constant. Moreover, the MA system showed no peak of the resistivity, and its resistivity was smaller than that of the MMA by an order of magnitude.

Film resistivity obtained from voltage-current curves by dynamic potential sweep technique.—On the assumption that Ohm's law is valid for the deposited film, the film resistivity was estimated using Eq. 1 and 2. It has been thought in an electropaint system that the film resistance showed nonohmic behavior because a high electric field of about 10^5-10^8 V/cm was applied to the film during deposition.[6,9,10] Beck measured voltage-current curves using the potential sweep technique with an anionic electropaint system to examine the influence of electric field on the deposited film.[9] Consequently, he proposed the space charge formation model to explain the nonohmic behavior of the deposited film. In addition, Cooke examined a variation in resistivity by suddenly changing the applied voltage from 200 to 100 V by using a film deposited on a steel panel at 200 V (20 μm thick, resistivity of 1.6 $\times$ 10^8 Ω cm).[10] His results did not conform to Ohm's law, and hence he considered that such changes were caused by the effect of the electric field. Beck[6] pointed out that reliable evaluation of the film resistance with a physical meaning can be achieved only from the following two measurements: an ac bridge technique using low voltage amplitudes, or a calculation from the residual current passed after deposition at constant voltage according to Ohm's law. Moreover, he described that the straight slope in the low voltage range, which is obtained from the potential sweep technique, is identical with the resistance measured by the ac bridge.

To check the validity of the resistivity calculated in the preceding sections, the ohmic behavior of the films was investigated. After

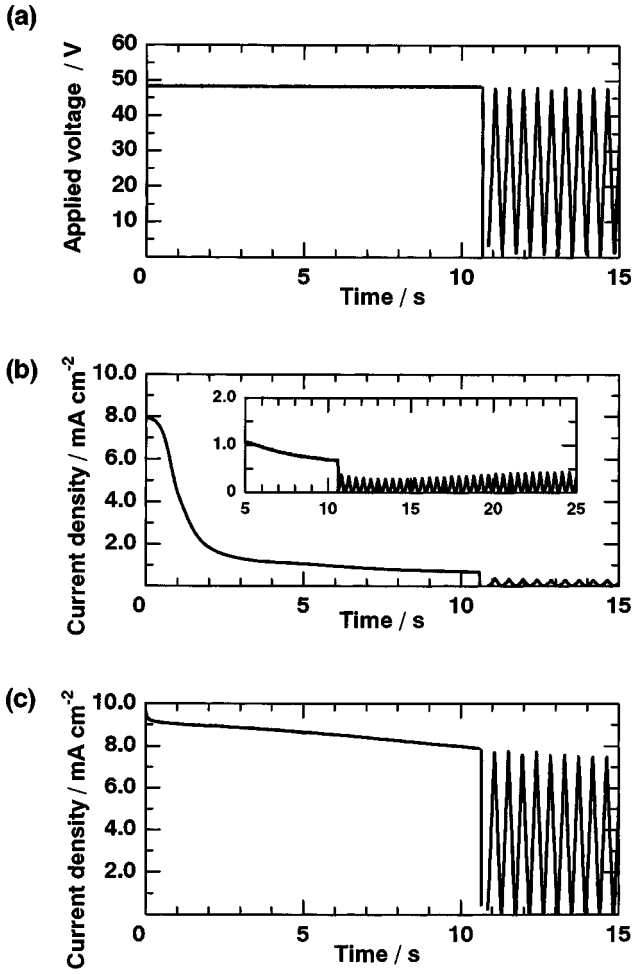

Figure 10. (a) Voltage-time profile when potential sweep technique was applied to a deposited film. First, the film was deposited at constant voltage for 10 s. Second, by switching from constant voltage to the sweep technique, the film deposition was continued. Conditions for the sweep mode are as follows: sweep rate 200 V/s, sweep voltage 0-50 V, and cycle number 35 times. (b) Current-time curve obtained from the MMA. Inset shows the full range of the measurement. (c) Current-time curve obtained from the MA.

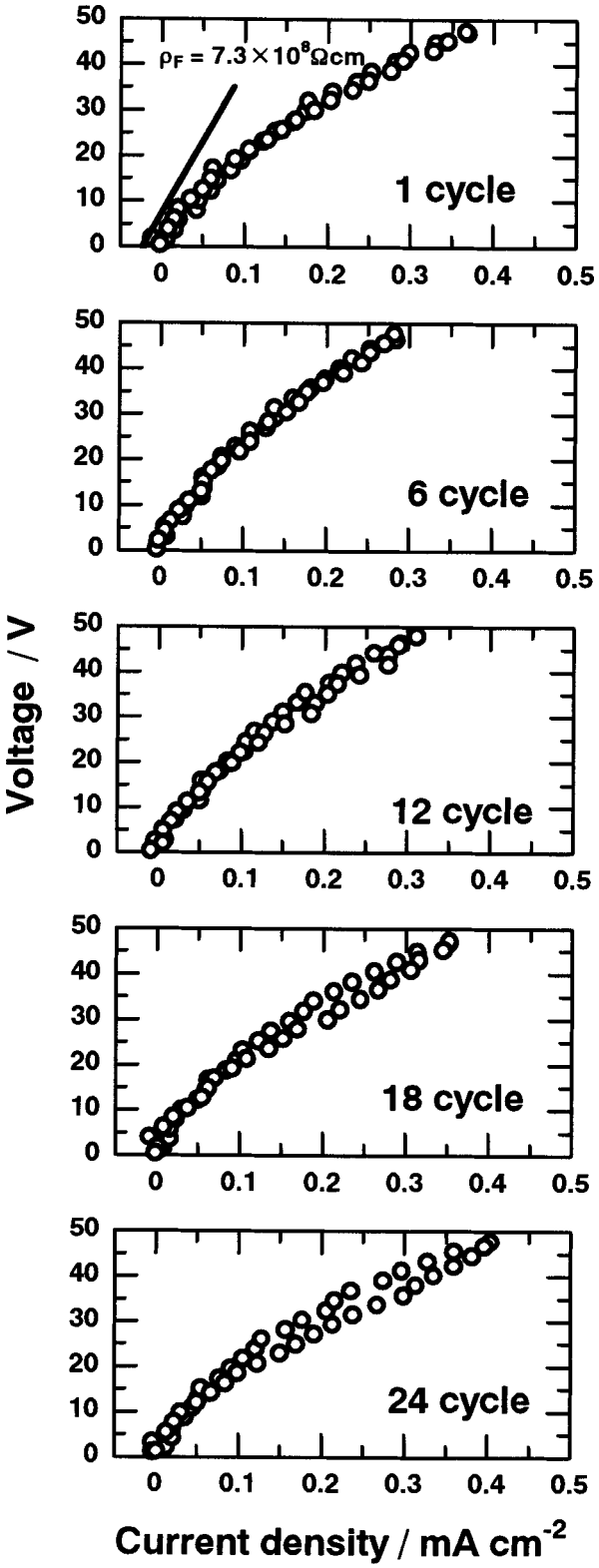

Figure 11. Voltage-current curves obtained from the MMA. Electrodeposition conditions are shown in Fig. 10.

being deposited at constant voltage (50 V), the film was electrolyzed 35 times using the potential sweep technique (the sweep rate of 200 V/s and the voltage cycle between 0 to 50 V). It took about 0.3 s to switch from the constant voltage to the sweep mode; in this case, the current was interrupted. Figure 10a shows a voltage-time curve applied to the system. During constant voltage deposition of 10 s, the MMA formed a film about 4 μm thick. The current-time curve for the MMA corresponding to Fig. 10a is shown in Fig. 10b. The figure revealed that the current fell off rapidly under constant voltage conditions, and then the peak current in the sweep mode was smaller than one-half of the current at 50 V just before switching to the sweep mode. While the sweep cycle was repeated, the peak current gradually decreased and again increased. Such behavior could be observed when the deposition time at constant voltage was shorter than 30 s. The deposition time exceeding 30 s at 50 V showed a monotonous decrease in the peak current.

However, the MA deposited a film about 10 μm thick at 50 V and for 10 s. The MA film decreased in current monotonously from the start of deposition. After the voltage was switched to the sweep mode, the peak current conformed to the trajectory which extended the current-time curve under constant voltage deposition (Fig. 10c). Figures 11 and 12 show the voltage-current curves for the MMA and the MA, respectively. For the MMA, the voltage was not proportional to the current, and then the deposited film displayed nonohmic behavior (Fig. 11). The hysteresis in the curves became greater as the cycle number increased. The film resistivity for the MMA was estimated to be 7.3×10^8 Ω cm from the straight slope through the origin, as described by Beck.[6] The results obtained from the constant voltage measurements in Fig. 3b were about 7.0×10^8 Ω cm at 10 s and agreed well with the estimation by the sweep technique. The

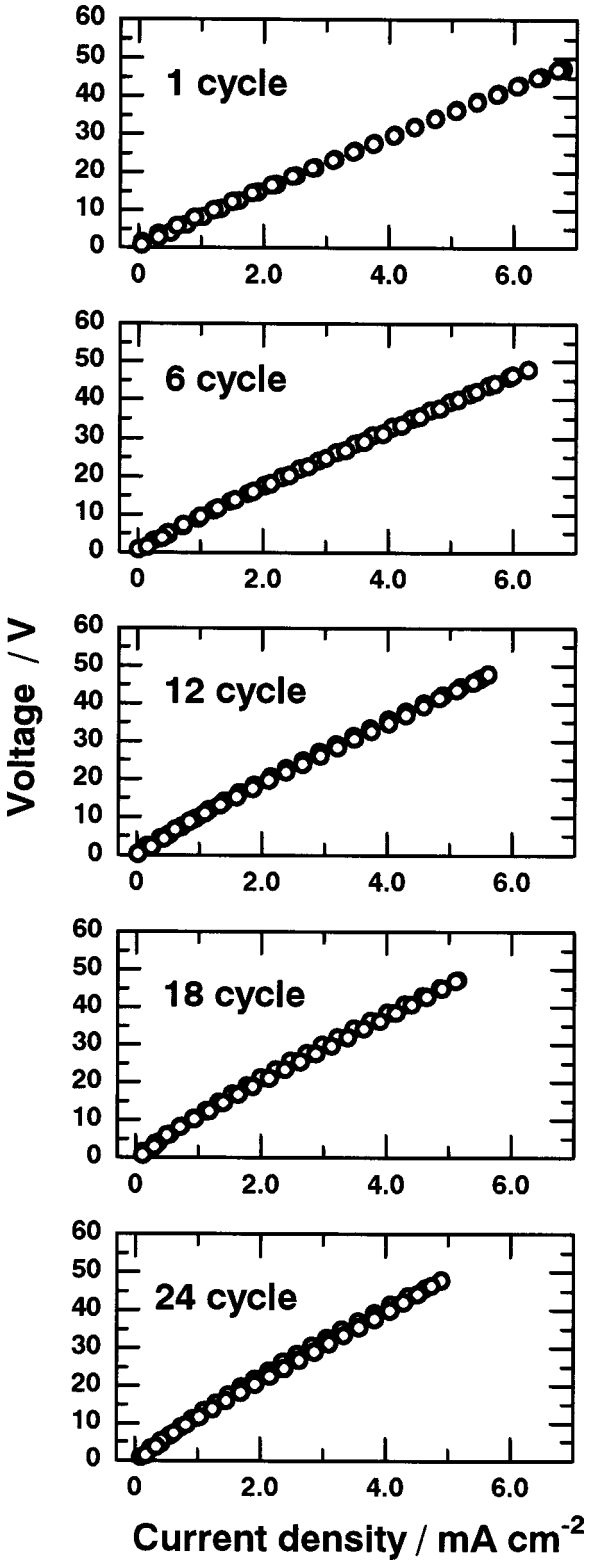

Figure 12. Voltage-current curves obtained from the MA. Electrodeposition conditions are shown in Fig. 10.

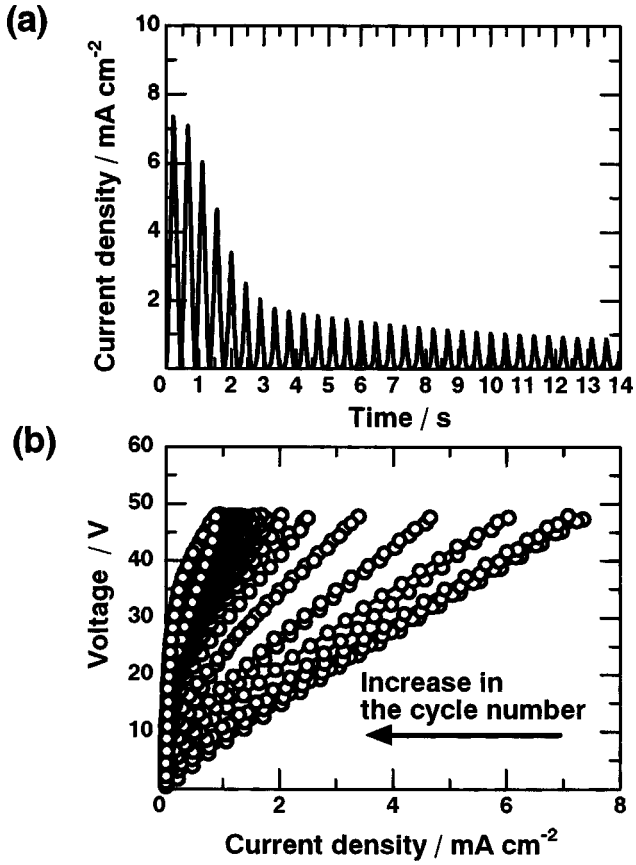

Figure 13. (a) Current-time curve of the MMA when electrodeposition was performed from the start of depostion using the potential sweep technique. (b) Voltage-current curves obtained from data shown in (a). Conditions for the sweep are as follows: sweep rate 200 V/s, sweep voltage 0-50 V, and cycle number 30 times.

voltage-current curves for the MA showed ohmic behavior, although they had a small deviation from the straight line after the 12th cycle (Fig. 12). The resistivity estimated from Fig. 12 was 0.7 $\times$ 10^7 Ω cm and was within the results calculated by Eq. 1. The evaluation of the film resistivity according to Ohm's law gives reliable results. Furthermore, the HRFF, such as in the MMA, produced a nonohmic film, and the IPFF, such as in the MA, created an ohmic film.

Influence of current interruption during deposition.—On switching from the constant voltage to the sweep mode, the peak current for the MMA film fell to about one-half of the current obtained under constant voltage deposition. We examined the deposition behavior using only the sweep technique. The current-time curves given in Fig. 13a showed a current decay similar to that obtained under constant voltage deposition. The values of the peak current obtained from the sweep technique were slightly large in comparison with the constant voltage deposition. Therefore, we confirmed that the sweep technique had no influence on the results shown in Fig. 10b. For the MMA, the fall in current in the sweep mode relates to the instantaneous current interruption: it needed about 0.3 s to switch from the constant voltage mode to the sweep mode. However, whenever a MA film deposited at constant voltage was left in the solution for 3-5 s with interrupting current, the subsequent electrolysis by the sweep technique resulted in a fall in the peak current of 5-10%. The thick MA film displayed such a tendency to decrease in current. The current interruption for both systems suggests that possibly the deformation of the film structure changed the film resistivity.

Discussion

The MMA and the MA differ in the deposition behavior and the electrochemical characteristics of the film. Both systems form a dense film at the early stage of deposition, and the film transforms into a spongy layer after growing to a certain thickness. The growth seems to follow the PF model.[5,6] We had considered that the film

formation progressed according to this model in the previous papers.[3,4] However, the model cannot fully account for the following phenomena. First, interruption of current varies the resistivity of the film. Second, a spongy layer with holes of several mm diam is formed. We discuss the film growth process, which can explain such phenomena.

Current path through a film.—As shown in Fig. 10b, by interrupting the current, the value of the current fell to one-half the value before the interruption for the MMA film. Moreover, a similar phenomenon also took place for the MA to some extent. A film formed by electrodeposition is a polymer, and hence current passed through the film is attributed not to electronic conduction but to ionic conduction. The current interruption influences the transport of ionic species in the film. Pores in the film contribute to the transport in the PF model. If the MMA follows this model, hydroxide ions migrate to the film/solution interface through pores and interstices between particles, and the film can grow. SEM observations of the MMA film showed a deposition morphology which is consistent with the PF model. Numerous pores existing in the film are 0.01-0.5 μm in diameter. If the pores dominated the mass transport, they would penetrate the film from the electrode surface to the film surface with a certain probability. We also had supported this idea in our previous papers.[3,4] However, to explain reasonably the influence of the current interruption by using the PF model, the pores must be deformed momentarily, and the migration of hydroxide ions must be obstructed. For latex, it is well known that compressive stress acts on the interstices between the particles by vaporizing water, and then the interstices coalesce.[11-13] For electrodeposition, a phenomenon similar to that in the latex is also caused because a film is deposited by changing from an aqueous solution of polymer to solid polymer. Moreover, particular phenomena in the electrodeposition are coalescence of film by Joule heating and an increase of stress by electro-osmosis.[5,6] Such phenomena should act on the film as an influence of the electrolysis or the electric field. It is difficult to assume such effects during current interruption. Furthermore, the probability of the pores penetrating the film from the electrode to the film surface should be extremely low because the polymer particles as a film are deposited at random. Thus, if the deposition mechanism of the MMA is explained by the PF model, the interstices between the MMA particles, which are observed with AFM, should contribute to mass transport. For the MA, the interstices between the MA particles cannot be observed with AFM, and hence we think that the transport of species generated by electrolysis occurs through the deposited layer itself: the MA forms an ion-permeable film. When electrodeposition was performed using a transparent cell made of glass, evolution of hydrogen gases could be seen from the film surface in both the MMA and the MA systems. These facts lead us to conclude that hydroxide ions and hydrogen gases migrate through the film. Hence, the question is whether the interstices between the MMA particles create a simple space layer or a continuous layer. If the interstices are the space filled with the electropaint solution, the influence of current interruption cannot be expected. However, such results cannot be obtained (Fig. 10b). We must consider from the experimental results that the interstices between the MMA particles form a continuous layer (or a coalescent layer) where the particles coalesced. Consequently, the MMA also follows IPFF where species are transported through the film itself. Such a viewpoint of the film growth results in the same growth mechanism for the MMA and the MA. We conclude that the current path during deposition is the film itself.

Difference of film resistivity in the MMA and the MA systems.—The resistivity of the MMA and the MA systems differs by an order of magnitude. The deposited film behaves as an ionic conductive film, and hence it is a certain solid electrolyte. Electrolytic concentration contained in the deposited film determines the resistivity. To confirm the characteristics of the film, we added phenolphthalein into the MMA and the MA. Electrodeposition was performed at constant voltage. The deposited film of the MMA showed a light pink color irrespective of the applied voltage, which suggests that its deposit was basic. However, the MA deposit was acidic without coloring the film pink. Moreover, we measured the concentration of lactic acid contained in the 20 μm film. The concentration in the MMA film was 6.3×10^{-3} mmol/g of deposited film, and the MA was 7.5×10^{-2} mmol/g. We reported that the MMA created a hydrophobic film and that the MA produced a hydrophilic film.[3] Such characteristics reflect the different concentrations. Thus, the film resistivity depends on the concentration of lactic acid.

For the MMA, the coalescent layer of particles has a different resistance from the particles themselves. That is, the inside of the particle composes an electrical insulating layer, and the coalescent layer around it comprises a conductive layer. Consequently, the coalescent layer acts as a practical current path. For the MA, the deposited film has a uniform resistivity because it contains a high concentration of lactic acid and has the structure of a flat surface without any particulate structures. Current can pass through the whole film of the MA. In comparison with the MA, the MMA film has low electronic conductivity; the current path is small because of the particulate structure. The difference between these structures affects the electrochemical characteristics during deposition, *e.g.*, the difference in applied voltage necessary for deposition. The model proposed here enables us to explain the difference in film resistivity for both systems. However, the influence of current interruption on the deposited film remains to be explained. Probably trace amounts of water in the film act upon such a phenomenon.

Pores formed in the film.—SEM observations showed that micropores of 0.05-0.1 μm were scattered in the MMA film with a thickness of 30 μm or less. The MA film was observed to be a non porous structure by SEM. Moreover, on increasing the film thickness, both systems formed holes of several mm diam, transforming the film morphology into a spongy layer. We consider such a transformation of the film morphology.

In general, the surface of a deposited film is covered with hydrogen gases generated by electrolysis of water when the film is taken out of a cell. The film rinsed with water immediately after deposition has a rough surface. This seems to be caused by the following. Hydrogen gases migrate to the film/solution interface through the film. Until hydrogen bubbles grow to a certain size, they are attached to the film surface depending on the surface roughness. We observed bubbles attached to a film surface when the film up to 30 μm was deposited for both systems. Once the MA film was taken out of its solution, the bubbles disappeared, and the film surface was covered with the solution. For the MMA, the bubbles stayed on the surface after the deposited film was taken out. Because the film surface of the MMA is composed of aggregates, its surface is rougher than that of the MA. Such a rough surface inhibits the bubbles from detaching. For a film at 30 μm or less, partial coverage by the bubbles allows the MMA to form pores of 0.05-0.1 μm diam. The formation of the micropores at a relatively thin thickness depends on the surface morphology of both systems.

The MA also showed an increase in surface roughness in the thickness range of 30-40 μm. The variation in the MA surface is due to the influence of the hydrogen bubbles. At a film thicker than 40 μm, the MA and the MMA transformed the deposit into a spongy layer. The surface of the spongy layer appears as holes rather than pores. The holes have a diam of 0.5-1 mm. In such a case, the film morphology of the MMA cannot be distinguished from that of the MA. If the film growth process conformed to the PF model, such great holes could not be produced. Consequently, surface coverage by hydrogen bubbles governs the formation of holes in the film and transforms the film structure (the hole formation is described in the next section in detail).

Phenomenon of film rupture.—A film rupture for both systems under constant current deposition takes place after the structure turns spongy with the growing film. The rupture occurs not at the electrode/film interface but within the film. In addition, under constant voltage conditions, the MMA does not produce ruptures, but

the MA causes them. The film rupture for the MA clearly depends on the film thickness. Another observation is that the film rupture takes place not at the edge of a substrate (high current density) but in the middle. There are three probable causes for the film rupture: hydrogen gases, the dielectric breakdown, and the sparking breakdown.[14,15] As shown in Fig. 4, the MMA system under constant current deposition showed that the electric field strength at the peak voltage was about 3×10^4 V/cm. The MMA film ruptures at 240-280 V. The film thickness in this case can be estimated to be about 30-43 μm. If a film rupture occurs at 35 μm and at 260 V, the electric field strength is estimated at 7.4×10^4 V/cm. In addition, a film rupture for the MA occurs at 25-35 V, in which the electric field is about 10^3 V/cm. The film rupture at low voltage suggests that the cause cannot be regarded simply as the effect of the electric field. It is appropriate to understand that the rupture is caused by hydrogen gases; nevertheless, the mechanism is difficult to prove experimentally from a microscopic viewpoint. However, the macroscopic results obtained from the experiments give us the following model for the film rupture caused by hydrogen gases. Constant current operation forcibly produces electrolytic products corresponding to the applied current. Hydrogen gases and hydroxide ions are transported through the film. Hydrogen gases coalesce as the bubbles reach the film surface. At the same time, the resin particles are coagulated with hydroxide ions and form the film. As the bubbles attach to the surface, the film grows around the bubbles. Hydrogen gases are confined in the film. Consequently, the bubbles form holes, and the spongy layer is deposited on a dense layer. The amount of hydrogen gases permeating the spongy layer cannot balance the amount produced at the electrode. When a deposited film covers a portion of the surface of the holes in which hydrogen bubbles are confined, the inner pressure rises; the film rupture takes place. The detachment of hydrogen gases from the surface depends on the convection of the solution, *e.g.*, by agitation or stirring. Thus, the film rupture is restricted to the middle of the substrate, as mentioned in the beginning of this section. The film rupture is a circumstantial evidence that hydrogen gases permeate the film.

Structure of the MMA film: Influence of film temperature during deposition.—Drazic *et al.* measured a temporal change in temperature at a film surface, using a cationic electropaint film deposited at constant voltage of 200-350 V.[16] According to their results, the surface temperature reached the maximum (40-85°C) at 20 s. Doroszkowski and Toynton also reported a rise in temperature at a film surface during deposition.[14] Deposition of the MMA film at 70-150 V and for 180 s raised the solution temperature by 0.3-0.5°C for 180 s. For the MMA, the Joule heat generated in the film influences the deformation of the film structure. Heating phenomena by electrolysis have been investigated in the fields of plating and anodic oxidation.[17-20] Hoshino and Boshin measured the surface temperature at a cathode during deposition using various plating solutions, and they analyzed the temperature change under natural convection conditions.[17] We applied Hoshino's analysis to an electropainted film to consider the influence of the Joule heat on the film deposition. The surface temperature of a film was estimated assuming that the physical constant of an electropaint solution is similar to that of water. Figure 14 shows the results of the surface temperature of a film, T_F, as a function of current density at various resistivities. The figure qualitatively explains the results which Drazic *et al.*[16] obtained, and a rise in temperature during deposition is suggested at a ρ_F of 10^8 Ω cm. For constant voltage deposition, the MMA requires a deposition voltage higher than the MA to attain the same thickness. The initial current during the MMA film deposition depends on the voltage value, 2.5 mA/cm^2 at 20 V and 14 mA/cm^2 at 100 V (Fig. 2). Therefore, once electrolysis of water is initiated, the MMA forms a film several micrometers thick. The MMA resin has a T_g of 70°C, and the deposited film begins to soften at a temperature near the T_g. Figure 14 suggests the possibility of the film attaining the softening temperature for a film resistivity of 10^8 Ω cm. As described in the section on current path through a film, we proposed

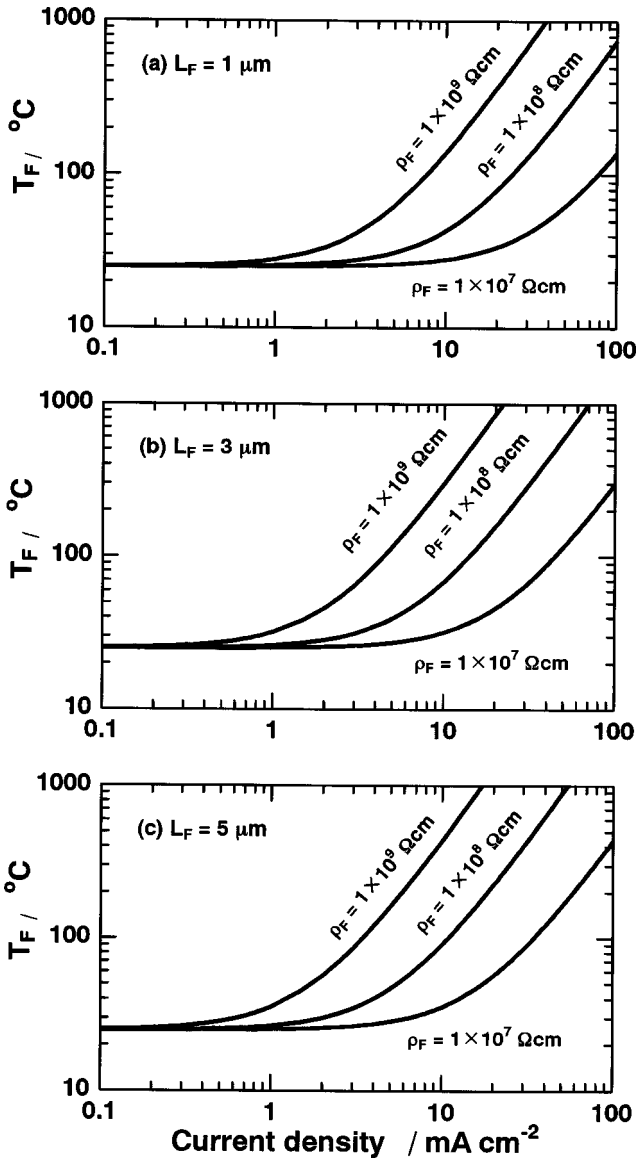

Figure 14. Estimation of temperature at a film surface, T_F, under natural convection condition. The T_F was shown as a function of current density at various values of resistivity.

the model in which the interstices between the particles create the continuous layer (the coalescent layer). When current passes through the coalescent layer, the Joule heat promotes coalescence of the interstices. The results of Fig. 3 exhibit the influence of the Joule heat. The progress of the coalescence at the interstices increases the film resistivity excessively, and then a portion of the film layer causes a kind of film rupture. Such variation is measured as a decrease of the resistivity with increasing voltage. However, the film is not perfectly broken down because the early deposited film becomes dense by the heat effect and behaves as a barrier-like and adhesive film (a dense layer). In such a dense layer, the interstices between particles promote coalescence so as to decrease the resistivity. In contrast, under constant current deposition, a current density lower than 1 mA/cm^2 has hardly any influence of the Joule heat on the film. The film is slowly deposited during the induction period of several seconds to form the dense layer of about 3 μm. After the 3 μm thickness is reached, the voltage abruptly rises. As in constant voltage deposition, a portion of the dense layer is broken down, and the resistivity peak appears. Consequently, the peak resistivity is independent of the current density (Fig. 5).

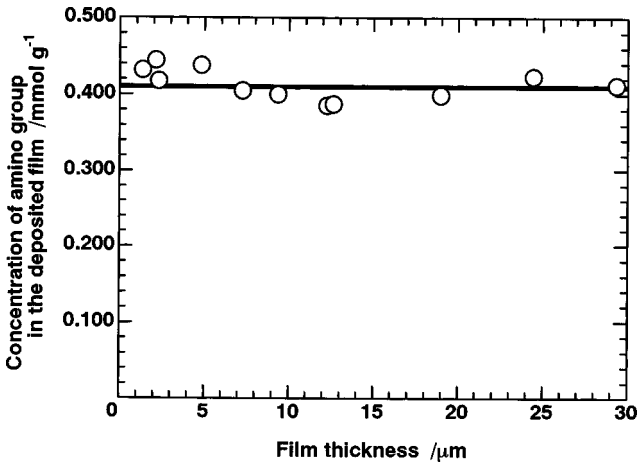

Figure 15. Concentration of amino groups contained in the MA deposit as a function of thickness. Electrodeposition was performed at constant voltage of 10 V, for various times, and at a solution temperature of 25°C. Solid line shows the calculated value of the concentration of amino groups from the MA composition: 4.1×10^{-1} mmol/g.

Film structure of the MA.—The MA, as shown in Fig. 9, gradually decreased in film resistivity with increasing thickness. All of our results support the model of IPFF: current passes through the deposited film, and the film growth takes place at the film/solution interface. Now, we must account for the change in resistivity for the MA. The change in the resistivity is expected to correspond to a change in the concentration of ionic species in the film. Because it can hardly be thought that the film composition changes depending on the deposition conditions, the concentration of amino groups in the film always remains constant. Thus, if concentration of lactic acid is low at the early stage, the relationship of such a change in the resistivity is established. To confirm this, the concentrations of amino groups and lactic acid in the MA film were determined (Fig. 15, 16). The concentration of amino groups was independent of the film thickness (Fig. 15). The concentration of lactic acid decreased with increasing thickness (Fig. 16). The resultant concentrations suggest that the MA film would be basic. However, the deposited film was acidic in another experiment, in which no color change was observed by adding phenolphthalein. This suggests that any lactic acid molecules do not dissociate in the deposited film. Lactic acid reacts with hydroxide ions at the electrode/film interface and forms lactate ions. Lactate ions formally migrate to the bulk solution through the film. However, hydroxide ions actually migrate in the film. Thus, we must understand that the MA has low resistivity because hydroxide ions have a high mobility.

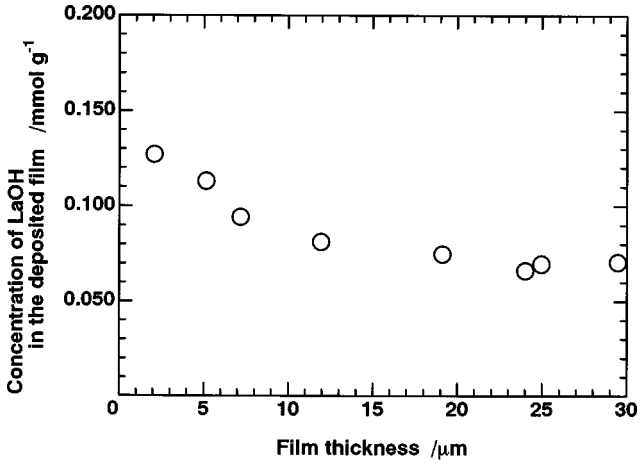

Figure 16. Concentration of lactic acid contained in the MA deposit as a function of thickness. Electrodeposition was performed at a constant voltage of 10 V, for various times, and at a solution temperature of 25°C.

Conclusions

We investigated the correlation of film formation with the film structure in electropaint systems, using two types of cationic resins with different T_g values: the MMA and the MA, 70 and 5°C, respectively.

The resistivity of the MMA (10^8-10^9 Ω cm) is higher by an order of magnitude in comparison with the MA (10^6-10^7 Ω cm). The voltage-current curves obtained using the potential sweep technique show that the MMA behaves as a nonohmic film and that the MA film exhibits ohmic behavior.

We proposed a new model for the MMA film formation, where current passed through the continuous layer itself. Thus, because the interstices between the MMA particles coalesce and form a continuous layer, the film growth for both systems follows the IPFF and can be practically explained by the same mechanism.

The film resistance depends on the concentration of lactic acid in the deposited film and the film structure. Moreover, at a film thinner than 30 μm, pores in the film are formed by the partial coverage of hydrogen gases at the film surface. The coverage transforms the structure of the deposited film, and then holes are formed with an increasing thickness of 30 μm or more. However, when a high resistance film like the MMA is deposited, the behavior of the film formation depends on the electrolysis mode: constant voltage or constant current deposition. The high resistance film is greatly influenced by the Joule heat under constant voltage deposition, but it is hardly affected under constant current deposition. Under constant current deposition, an induction period was observed for the MMA, in which the film grew and the voltage rose. Thus, the induction period is defined as the time when the film with a certain resistivity is formed.

Acknowledgments

The authors thank Professor F. Hine, Nagoya Institute of Technology, for useful comments. We also acknowledge the advice on this manuscript from Dr. Y. Suzuki, Central Laboratory of C. Uyemura & Co., Ltd.

C. Uyemura & Co., Ltd. assisted in meeting the publication costs of this article.

References

1. N. Furuno and Y. Ohyabu, *Prog. Org. Coat.*, **5**, 201 (1977).
2. N. Furuno, H. Kawai, and Y. Ohyabu, *J. Jpn. Soc. Colour Mater.*, **42**, 362 (1969).
3. Y.-I. Suzuki, H. Fukui, K. Tsuchiya, S. Arita, and Y. H. Ogata, *Prog. Org. Coat.*, **42**, 209 (2001).
4. Y.-I. Suzuki, H. Fukui, K. Tsuchiya, and Y. H. Ogata, *J. Electrochem. Soc.*, **147**, 3700 (2000).
5. P. E. Pierce, *J. Coat. Technol.*, **53**, 54 (1981).
6. F. Beck, *Prog. Org. Coat.*, **4**, 1 (1976).
7. S. Maeda, T. Asai, and H. Okada, *Corr. Eng. Jap.*, **36**, 268 (1982).
8. V. B. Miskavic and M. D. Maksimovic, *Surf. Coat. Technol.*, **26**, 353 (1985).
9. F. Beck, *Ber. Bunsenges. Phys. Chem.*, **72**, 445 (1968).
10. B. A. Cooke, *Paint Technol.*, **34**, 12 (1970).
11. G. Brown, *J. Polym. Sci.*, **22**, 423 (1956).
12. F. Lin and D. J. Meier, *Prog. Org. Coat.*, **29**, 139 (1996).
13. M. Visschers, J. Laven, and A. L. German, *Prog. Org. Coat.*, **30**, 39 (1997).
14. A. Doroszkowski and M. A. Toynton, *Prog. Org. Coat.*, **17**, 191 (1989).
15. R. E. Smith and D. W. Boyd, *J. Coat. Technol.*, **60**, 77 (1988).
16. D. M. Drazic, N. M. Acamovic, and O. D. Stojanovic, *J. Coat. Technol.*, **66**, 27 (1989).
17. S. Hoshino and R. Boshin, *J. Met. Finish. Soc. Jpn.*, **24**, 567 (1973).
18. S. Hoshino and R. Boshin, *J. Met. Finish. Soc. Jpn.*, **25**, 504 (1974).
19. S. Hoshino and R. Boshin, *J. Met. Finish. Soc. Jpn.*, **27**, 145 (1976).
20. T. Imamura, S. Hoshino, and S. Matsumoto, *J. Met. Finish. Soc. Jpn.*, **28**, 101 (1977).